phosphor and CCD camera combination.

Fig.L.8.1 shows a schematic of the experimental setup used to measure the electron beam profile. At a gas jet pressure of 37 bar and laser intensity of ~2 x 10^{18} W/cm^2, a collimated beam of electrons with a low-divergence (~10 mrad), with few tens of MeV energy was observed. A typical electron beam profile recorded on DRZ phosphor screen is shown in Fig.L.8.2.

The experiments were carried out using the 10 TW Ti:sapphire laser facility at RRCAT. This provides laser pulses of maximum energy of about 450 mJ in 45 fs pulses. The laser beam was focussed on a helium gas jet using a 40 cm focal length gold coated off-axis parabolic mirror. The gas jet was produced by a shock wave-free slit type (10 mm x 1.2 mm) supersonic Laval nozzle. Helium gas was puffed using a fast solenoid valve and its density was varied by changing the backing pressure of the gas. The Ti:Sapphire laser beam was focussed at the entrance edge of the gas jet, about 1.5 mm above the nozzle entrance. The focal spot diameter of the beam was 18μm (FWHM).

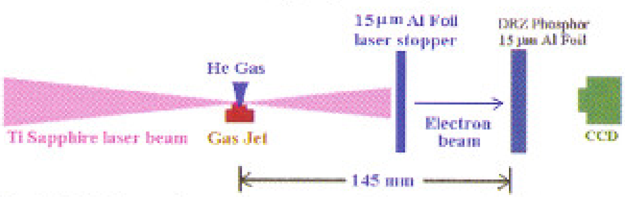

Fig.L.8.1: Set-up for measurement of beam profile of the laser accelerated electrons.

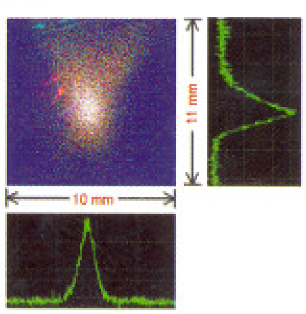

Fig.L.8.2: Electron beam profile recorded using DRZ phosphor, on a CCD camera.

Contributed by:
P.A. Naik (panaik@cat.ernet.in) and A. Moorti

L.9 Improving performance of porous silica sol-gel anti-reflection coated optics for high power Nd: glass laser

Porous silica sol-gel coated optics is used in high power laser systems because it has high laser induced damage threshold (LIDT) and has high spatial uniformity over large diameters. High power laser systems have MOPA (master oscillator power amplifier) architecture and use sequential optical relaying using vacuum spatial filters to overcome laser wavefront distortions caused by self-focusing of the laser at high intensities. In order to use the sol-gel AR coated optics in spatial filters, the degradation of optical performance and LIDT of the coatings at the laser wavelength upon exposure to the vacuum oil vapours is an important consideration. Laser Plasma Division of RRCAT has developed a technique using hexamethyl-disilazane (HMDS) vapour treatment of the coatings to overcome the degradation of optical performance [R. Pareek et al Optical Engineering (in press)] of sol-gel AR coatings. The degradation in the optical quality of the coatings occurs mainly due to the adhesion of contaminant vapours to the polar silica nano-particles in the coatings. The polar nature of the silica coatings can be reduced if the coatings are exposed to HMDS vapours. This may prevent the degradation of the coatings upon exposure to contaminant vacuum oil vapours.

Two sets of single layer AR coatings, namely silica and ammonia and HMDS treated porous silica were prepared and exposed to rotary pump oil vapours in a vacuum chamber. Fig.L.9.1 shows the reflection spectra of a) porous silica coating, and b) the same coating exposed to oil vapours. It is seen that for the silica coating not exposed to oil vapours, the spectrum has a minimum of its reflectivity spectrum at λ_{min} = 1054 nm (lasing wavelength) with a reflectivity of R = 0.26%. It is also observed from Fig.L.9.1b that the minimum of reflectivity shifts to a higher wavelength by 122 nm as compared to the minima of the coating not exposed to oil vapours. A substantial degradation of the reflectivity occurs for vapour exposed silica coating giving a reflectivity of 2.1% at 1054 nm in comparison to the 0.26% reflectivity of the coating not exposed to oil vapours.

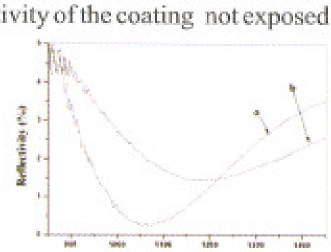

Fig.L.9.1: Reflection spectra of a) porous silica coating and b) the same coating after exposure to oil vapour.

Figure L.9.2 shows reflection spectra of a) a porous silica coatings treated with ammonia and HMDS, and b) the same coating exposed to oil vapours. It can be seen that there is only a marginal shift of ~20 nm of the λ_{min} value between the oil vapour exposed and un-exposed coatings that were treated with ammonia and HMDS. The shift in the minima of the spectra of treated coatings is much smaller than that of untreated coatings in Fig.L.9.1. The change in reflectivity of the oil vapour exposed and unexposed HMDS treated coatings is small (~0.01). It was also observed that the ammonia and HMDS treated coatings have a higher LIDT at the lasing wavelength in comparison to untreated coatings after exposure to the oil vapour. This finding agree well with the measurements of imaginary part of refractive index at 1054 nm.

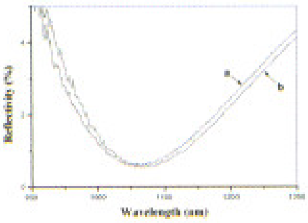

Fig.L.9.2: Reflection spectra of a) porous silica coating treated with ammonia and HMDS and b) the same coating after exposure to oil vapour.

Contributed by:
R. Pareek (rpareek@cat.ernet.in) and A. S. Joshi

L.10 High voltage programmable ramp generator for high speed streak camera

Streak camera is a high speed recording instrument, used as a diagnostic tool for studying very fast events, especially in the field of intense laser-matter interaction. Streak camera consists of a streak tube which has a photocathode, deflecting plates and a phosphor screen. When the light from the event is incident on photocathode, it generates photoelectrons, which are deflected by deflecting plates and an image is generated on the screen. For this reason, streak camera requires a high voltage and fast ramp generator of amplitude of +/- 500 V and rise time of 1 ns. However, it is also necessary to vary the slope of this ramp so that the event can be analyzed properly. In this article, we have presented a high voltage ramp generator with programmable slope and microprocessor based control, developed for this purpose. The ramp generator consists of a high voltage step generator, followed by an integrator. The components of the integrator are designed such that they can be varied by a microcontroller. The unit generates two bipolar ramp voltages with fastest speed of < 1ns and provides continuous slope variation from 6 ns to 30 ns for a ramp voltage of 500 V. This is developed by Laser Electronics Support Section, RRCAT as a part of automation of streak camera.

The step voltage is generated by two stacks of avalanche transistors connected in series to minimize the jitter. The stacks are biased by applying positive ramp bias at one end of the first stack and negative ramp bias at the other end of the second stack. Both the stacks are triggered through a pulse transformer having one primary and two secondary windings (1:1:1). The outputs thus generated are connected to two integrator units through two high voltage dc relays. By activating these relays, the step voltages can be connected to the integrator units, thus getting slower slope of ramp voltages decided by the value of R, L, and C.

Variable and high voltage capacitor and inductor required for this unit and which can be controlled by microprocessor were developed in-house. For variable C, a gang capacitor with two identical capacitors variable from 47 pF to 253 pF was used. The shaft of the same is rotated by a stepper motor. For variable L, two solenoid coils are used and the inductances are varied by moving the ferrite cores by another stepper motor. The inductances vary between 3 μH to 15 μH. A resistor of 110 Ω is used for all the values of L and C as it provides overall satisfactory performance. A photograph of the variable slope ramp generator module showing its constructional features is shown in Fig.L.10.1. Fig.L.10.2 shows the ramp output waveforms with variable L and C.

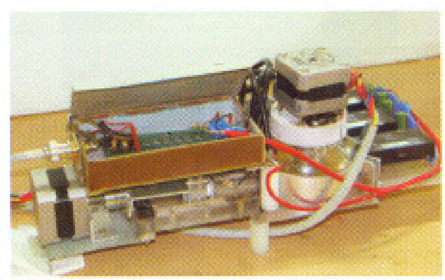

Fig.L.10.1: Programmable high speed ramp generator module.

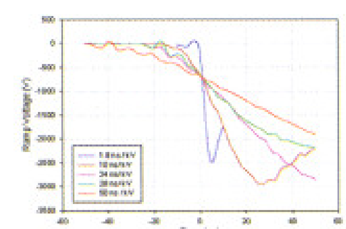

Fig.L.10.2: Variable slope ramp output wave forms.

For controlling various operations of the ramp generator, a micro controller ADμC831 (Analog Devices) is used. This microcontroller is programmed to drive both stepper motors described above and is interfaced to the PC using RS232 link. A LABVIEW based graphical user interface (GUI) is developed in personal computer for operation of the instrument.

In fastest mode, two step voltages with < 1ns rise time are generated. The rise time is calculated for a variation of 500 V in linear part of the ramp. The ramp speed can be adjusted to any desired value within the range 6 ns to 30 ns by changing L and C, with the help of stepper motors.

Contributed by:
J. Upadhyay (janky@cat.ernet.in) and C.P. Navathe